Published in final edited form as:
J Biol Chem. 2006 June 2; 281(22): 15194–15200. doi:10.1074/jbc.M513809200.

MODULATION OF VOLTAGE-DEPENDENT *SHAKER* FAMILY POTASSIUM CHANNELS BY AN ALDO-KETO REDUCTASE

Jun Weng[*], **Yu Cao**[*], **Noah Moss**, and **Ming Zhou**
Department of Physiology and Cellular Biophysics College of Physicians and Surgeons Columbia University New York, NY 10032

Abstract

The beta subunit (Kvβ) of the *Shaker* family voltage-dependent potassium channels (Kv1) is a cytosolic protein that forms a permanent complex with the channel. Sequence and structural conservation indicates that Kvβ resembles an aldo-keto reductase (AKR), an enzyme that catalyzes a redox reaction using a nicotinamide adenine dinucleotide phosphate (NADPH) cofactor. A putative AKR in complex with a Kv channel has led to the hypothesis that intracellular redox potential may dynamically influence a cell's excitability through Kvβ. Since the AKR function of Kvβ has never been demonstrated, a direct functional coupling between the two has not been established. We report here the identification of Kvβ substrates, and the demonstration that Kvβ is a functional AKR. We have also found that channel function is modulated when the Kvβ-bound NADPH is oxidized. Further studies of Kvβ's enzymatic properties seem to favour Kvβ's role as a redox sensor. These results suggest that Kvβ may couple cell's excitability to its metabolic state, and present a new avenue of research that may lead to understanding of Kvβ's physiological functions.

Kv channels control the flow of K^+ through the cell membrane in response to changes in membrane potential. Opening of the channel causes membrane hyperpolarization that can curtail excessive membrane excitability or simply tone down normal membrane activity. Kvβ, found in plants, insects, and mammals, attaches to the cytosolic face of the Kv1 channels to form a macromolecular complex (Figure 1A)([1-5]). There are three mammalian Kvβ genes (Kvβ1-3)([6,7]), and all Kvβs have a conserved core region with sequence similarities to an AKR ([8,9]). The structure of the conserved core of a Kvβ, Kvβ2 from rat, shows that it has a canonical AKR fold, with highly conserved catalytic residues in the correct geometry for catalysis to happen, and has a nicotinamide cofactor tightly bound (Figure 1B)([3,10,11]). These features suggest that Kvβ is a functional AKR. In many cells, acute changes in Kv channel current have long been observed when cellular redox state is altered, for example, under hypoxic condition or oxidative stress ([12-17]), but the redox sensing mechanism remains unknown. Could Kvβ be the missing link between cellular redox chemistry and Kv channel activities? In this study, we address the questions of whether Kvβ is a functional AKR, and whether the AKR function is coupled to channel functions.

AKRs catalyze the reduction of an aldehyde to an alcohol by oxidizing an NADPH cofactor. Most AKRs have a broad substrate spectrum so that in addition to their native substrates, they also convert small-molecule aldehydes such as benzaldehyde derivatives([18]). The catalysis follows a kinetic mechanism shown in Scheme I. An AKR, E, binds sequentially an NADPH and an aldehyde substrate([19]) to form a ternary complex, E-NADPH-aldehyde. The redox

Address correspondence to: Ming Zhou, Department of Physiology and Cellular Biophysics, Columbia University College of Physicians and Surgeons, 630 West 168th Street, New York, NY 10032; Tel: 212-342-3722; Fax, 212-305-5775; mz2140@columbia.edu.
*These authors contributed equally to this work.

reaction then occurs when the enzyme helps transfer a hydride from the cofactor to the aldehyde. The product, an alcohol, dissociates from the enzyme and is followed by the oxidized cofactor $NADP^+$. Many AKRs show high specificity to NADPH over its close relative, nicotinamide adenine dinucleotide (NADH)([18]). The hydride transfer step is usually fast, and the nucleotide exchange steps, or the protein conformational changes associated with them, are slow and rate-limiting([20,21]). The cycle in scheme I is reversible so that an alcohol can be oxidized to an aldehyde accompanied by the conversion of an $NADP^+$ to NADPH.

EXPERIMENTAL PROCEDURES

Molecular biology and mutagenesis

For protein expression, rat Kvβ2 (accession number: CAA54142, residues 36 to 363) was cloned into a pQE70 vector (Qiagen) between the SphI and BamHI sites with a C-terminus 6-histidine tag. For electrophysiological measurements, rat Kv1.4 (accession number: CAA34133) or Kvβ2 was cloned into a modified pBluescript vector for *in vitro* transcription. Mutations were made using the QuikChange (Strategene) kit and verified by sequencing through the entire coding region.

Protein expression and purification

XL-1Blue cells were used to express protein. Cells were grown in Luria broth at 37°C to an O.D. of ~1.2 and induced with 0.5 mM IPTG (final concentration). Immediately after induction, the temperature was reduced to 20°C and cells were harvested 16 hours after induction. Expressed protein was purified on a Talon Co^{2+} affinity column (BD Sciences). Throughout the purification procedure, the following buffer was used: 20 mM Tris pH 8.0, 300 mM KCl, 10% (volume:volume) glycerol, and 1mM β-mercaptoethanol. Non-specifically bound protein was washed using 20mM imidazole added to the above solution and Kvβ2 protein was eluted with 300mM imidazole. Immediately after elution, the affinity tag was removed by a brief incubation with trypsin at a Kvβ2 to trypsin ratio of ~ 150:1 (w:w). The protein was then loaded onto a Superdex 200 column (Amersham) for final purification. The column was equilibrated with the reaction buffer: 150mM KCl, 20mM Tris, pH 8.0. Protein concentration was determined using the BCA kit (Pierce).

Enzyme kinetics measurement

To measure the steady-state multiple turnover reaction rate, the reaction mixture (100μl) contains 0.2mM NADPH, 30μg Kvβ2 protein, and desired concentration of substrates in the reaction buffer. The reaction mixture was incubated at 37°C and NADPH (ε_{340}=6.22 $mM^{-1}cm^{-1}$) absorption was monitored at 340nm using a PharmaSpec UV-1700 (Shimadzu) equipped with a temperature controlling unit (CPS-240A). The reaction was initiated by the addition of a substrate. The initial turnover rate constant was calculated from the linear part of the decrease in the absorbance. Blank controls with no protein were incorporated routinely and the background NADPH consumption was subtracted.

As a positive control, we obtained rat 3α-hydroxysteroid dehydrogenase protein (a gift from Dr. Trevor Penning, University of Pennsylvania), and measured its specific activity using the following conditions: 75 μM androsterone (dissolved in acetonitrile), 2.3 mM nicotinamide adenine dinucleotide (NAD^+), 100mM potassium phosphate (pH 7.0), and 4% acetonitrile (total). We initiated the reaction by adding the enzyme and monitored the absorbance at 340nm over time. We obtained a specific activity of 1.4 ± 0.1 μM (n=5) of androsterone oxidized per minute per milligram of protein, similar to the value of 1.6 μM $min^{-1}mg^{-1}$ obtained in Dr Penning's lab.

To measure the single-turnover hydride transfer reaction rate, Kvβ2 protein was concentrated to 3-10 mg/ml, mixed with proper concentrations of substrates, and the absorption at 363nm was followed over time at 37°C. The 23nm red shift of the absorption peak for the bound NADPH is likely caused by interactions between the nicotinamide ring and the surrounding residues. Previous studies have demonstrated that the 363nm peak is due to the bound NADPH ([22]). The fraction of NADPH remaining on Kvβ was then plotted versus time and the data points were fit with a single exponential function in Origin (Microcal Inc). The inverse of the exponential time constant is defined as the hydride transfer rate constant. When higher than 5mM 4-CB was used in either the multiple or single turnover measurement, 40mM Tris was used to maintain the solution pH at 8.0.

Channel expression and electrophysiology

mRNA was prepared by *in vitro* transcription and purified using the Trizol reagent (Invitrogen). mRNAs were injected into Xenopus oocytes for channel expression. For co-expression, Kv1.4 and Kvβ2 mRNAs were injected at a ratio of 1:3 (w:w). The wild type Kv1.4 has a cysteine residue at position 13 that can be oxidized on inside-out patches to affect channel inactivation, and a C13S mutant or addition of dithiothreitol (DTT) abolishes this effect([23]). To eliminate concerns that the change in inactivation could be due to cysteine oxidation, we used the C13S Kv1.4 in this study. In parallel, we also tested 4-CY and 4-CB on Kv1.4 wild type co-expressed with Kvβ2, in the presence of 5mM DTT, and essentially the same results were obtained.

We recorded patch-clamp currents from oocytes 3-5 days after injection. Electrodes were drawn from patch glasses (G85150T-4, Warner Instruments) and polished (MP-803, Narishige Co.) to a resistance of 0.6-1MΩ. The pipette solution contained (in mM): KCl 130, $MgCl_2$ 2, and KH_2PO_4 10 at pH 7.4. The bath solution contained (in mM): KCl 80, EGTA 5, and KH_2PO_4 50 at pH 7.4. pH was adjusted with KOH. The higher buffer content in the bath solution is necessary to maintain the pH at 7.4 for 5mM or higher 4-CB. K^+ currents were elicited by holding the patch at −100mV for at least 30 seconds and stepping to +60mV for 500 miliseconds. The volume of the recording chamber (Warner Instruments) is approximately 120μl and complete exchange of solution was achieved by perfusing 1ml of new solution by gravity flow with a flow rate of 2-3ml/minute.

Inactivation of Kv1.4 with or without Kvβ2 has been studied extensively ([24-28]). Current inactivation can be fit by an exponential function with two components. The faster component, which is also the predominant one, is mainly contributed by the N-type inactivation ([29]), and the slower component is thought to be mainly due to the C-type inactivation ([27,30]). Here we follow the same tradition to quantify channel inactivation. For Kv1.4 co-expressed with the wild type Kvβ2, both the slow and fast inactivation time constants were modulated by 4-CY (Table 1). Since the N- and C-type inactivations are tightly coupled, we do not know yet if the change in the slow component is due to a direct effect on the C-type inactivation or a result of change in the N-type inactivation. We focused on the fast component and we defined the inverse of the smaller time constant as the rate constant of channel inactivation, and used the rate constant as a measure for the effect of Kvβ substrates.

Chemical Reagents

All chemical reagents were purchased from Sigma, except for 4-oxo-nonenal (Cayman chemicals). Substrates were first prepared in ethanol (4-CY) or dimethyl sulfoxide (4-CB) and then diluted to the desired final concentration. The final concentration of ethanol or dimethyl sulfoxide is less than 1% in electrophysiological measurements. NADPH was purchased as a tetra-sodium salt. Since sodium ions block potassium channels from the intracellular side, we exchanged the sodium to potassium ions by FPLC and the stock solution was aliquoted and stored at −80°C.

RESULTS

Single turnover enzymatic reactions

Freshly purified Kvβ2 protein contains the reduced form of the cofactor (NADPH), as indicated by a 363nm peak in the UV absorption spectrum (Figure 2A), and the occupancy of NADPH is more than 90%([10,22]). Since $NADP^+$ has little absorption at the same wavelength, the NADPH-to-$NADP^+$ conversion eliminates the 363nm-peak. Utilizing this as a readout, we screened small-molecule aldehydes which are common AKR substrates. We have identified several potential Kvβ substrates and two of the compounds, 4-carboxybenzaldehyde (4-CB) and 4-cyanobenzaldehyde (4-CY) (Figure 2B, inset), were used here to study Kvβ's enzymatic activity and substrate-induced channel modulations.

Shown in Figure 2B are UV spectra recorded at the indicated time points after mixing Kvβ2 protein with 5mM 4-CB. The peak at 363nm decreases over time, and the reduction of the peak reflects the oxidation of the Kvβ2-bound NADPH. Since no free NADPH was added, this is a single turnover reaction. When the fraction of NADPH remaining was plotted versus time (Figure 2C), the data points were well fit by a single exponential function with a time constant of 8.4 ± 0.1 minute (Figure 2C), consistent with a single-step hydride transfer reaction. Similar results were obtained when 5mM 4-CY was used, but with a smaller time constant of 2.3 ± 0.05 minute (Figure 2C), indicating that 4-CY at 5mM concentration consumes the bound cofactor ~3 fold faster than 4-CB.

To support the conclusion that the observed NADPH consumption is due to an enzymatic reaction, three control experiments were done. First, free NADPH was mixed with 5mM 4-CB in the absence of Kvβ2 protein and the change in NADPH absorption was monitored over time. A very slight decrease of NADPH absorption was observed over a period of one hour (Figure 2D), indicating that the reaction is greatly facilitated when the cofactor binds to the Kvβ2 protein.

Second, an active site residue, aspartate 85 (Figure 1B), was mutated to an asparagine (N) and the D85N mutant protein was expressed and purified. D85 is highly conserved in all AKRs, and a D-to-N mutation reduces the rate of catalysis in other AKRs such as aldose reductase and 3α-hydroxysteroid dehydrogenase (3α-HSD) by ~12 and 31 fold, respectively([31,32]). The purified D85N Kvβ2 protein has a bound NADPH cofactor, as indicated by an absorption peak near 360nm. When the D85N mutant protein was mixed with 5mM 4-CB, the absorption of the bound cofactor changed very slowly with a time constant of 330 ± 20 minute (Figure 2C, see also Figure 3A). The time constant is ~40 fold slower than that of the wild type Kvβ, indicating that the mutation slowed down the enzymatic reaction. This result supports the conclusion that Kvβ is a functional AKR.

Third, the reverse reaction, that is, transfer of a hydride from an alcohol to an $NADP^+$, was tested. To do this, we purified the oxidized Kvβ2, i.e., Kvβ2 protein after its bound NADPH was consumed by 4-CY, by passing the reaction mixture through a size exclusion column. Interestingly, we found that the elution does not contain a peak corresponding to $NADP^+$, which should be easily detected (Figure 2E). This indicates that the oxidized cofactor ($NADP^+$) stays tightly bound to Kvβ2. Using the oxidized Kvβ2, we screened small-molecule alcohols for their ability to reduce the bound cofactor and we found potential substrates. Result from one of them, 4-methoxybenzalcohol (4-MOB), is shown in Figure 2F. When 4-MOB (10mM) was mixed with the oxidized Kvβ2, absorption at 363nm gradually increased (Figure 2F inset) and recovers to approximately the same level as freshly purified protein. The time course of NADPH generation was well fit with a single exponential function ($\tau = 61 \pm 1$ minute, Figure 2F), consistent with a single step hydride transfer reaction. The consumption and the

re-generation of the Kvβ2-bound NADPH by small-molecule aldehydes and alcohols clearly demonstrated that Kvβ is a functional AKR.

Single versus multiple turnover enzymatic reactions

To further characterize the hydride transfer reaction, we measured the rate constant of the bound NADPH consumption, i.e., the single turnover reaction, at different 4-CY or 4-CB concentrations. We found that the rate constant increases with either 4-CB or 4-CY concentration, and does not reach saturation even at 20mM of a substrate (Figure 3A, left panel). As a control, we used the D85N Kvβ2 protein and measured its hydride transfer rate at three different 4-CB concentrations (Figure 3A, right panel). The rate is much slower than that of the wild type at all three substrate concentrations (2, 5, and 10mM), supporting the conclusion that that Kvβ is a functional AKR.

It is remarkable that the rate constant-concentration does not reach saturation. This indicates that both substrates have low occupancies on the enzyme so that binding is not saturated, something that is expected because both compounds are not native substrates. More importantly, it indicates that Kvβ is capable of converting the bound NADPH at a rate equal to or faster than $1.9 + 0.06$ minute^{-1} (20mM 4-CY), a time scale that is physiologically relevant in terms of redox sensing in a cell([33]).

The hydride transfer step is only a half-reaction in the enzymatic reaction cycle, so we next measured the steady-state turnover rate constant for the cycle shown in Scheme I. The turnover rate constant was plotted versus 4-CB or 4-CY concentrations (Figure 3B), and the data points were well fit by a Michaelis-Menten equation with a maximum turnover rate constant of 0.073 ± 0.0016 and 0.082 ± 0.0011 /minute, and a Km of 3.2 ± 0.17 and 2.7 ± 0.12 mM, for 4-CB and 4-CY, respectively. When NADPH was substituted with NADH, no turnover was observed (data not shown), indicating that Kvβ has evolved to use specifically NADPH for catalysis. The steady-state turnover rate constant for both 4-CB and 4-CY is approximately the same but is much slower than the hydride transfer rate constant, especially for 4-CY. This is consistent with a reaction mechanism in which the cofactor exchange steps are rate-limiting. Since the cofactor exchange steps are not substrate dependent, it suggests that the steady-state turnover rate constant is similar even when Kvβ catalyzes its native substrate(s). This property may have important physiological implications (see Discussion).

As an additional control and to further support the conclusion that Kvβ is an AKR, we mutated another highly conserved catalytic site residue, K118 (Figure 1B), to a methionine. A K-to-M mutation in rat 3α-HSD reduces the multiple turnover rate by more than 1000 fold ([32]). We expressed and purified the K118M mutant Kvβ2, and measured the multiple turnover rate constant at three different 4-CY concentrations (Figure 3B). At 5 mM 4-CY, the turnover rate constant ($(1.04 \pm 0.21) \times 10^{-4}$ minute^{-1}) was ~500 fold slower than that of the wild type (0.053 ± 0.003 minute^{-1}). The rate is essentially indistinguishable from that of free NADPH oxidation without the presence of a Kvβ protein. This result indicates that the conserved lysine is important for catalysis, and reinforces the conclusion that Kvβ is a functional AKR.

Channel modulation by Kvβ substrates

That Kvβ is a functional AKR naturally leads to the question of whether the redox reaction on Kvβ affects channel function. To address this question, we co-expressed Kv1.4 with Kvβ2, and monitored channel function on inside-out patches before and after applying a Kvβ substrate.

Figure 4A shows currents from a typical inside-out patch excised from an oocyte co-expressing Kv1.4 and Kvβ2. When 4-CY was perfused on the intracellular side of the membrane, channel

inactivation rate decreased from 81 ± 1.9 sec^{-1} to 46 ± 1.4 sec^{-1} (Figure 4A & E, and Table 1; n=31 patches from 8 batches of oocytes), and both the peak current and the steady state current levels increased significantly (Figure 4A). 4-CB induced an almost identical response (data not shown). We have observed the substrate-induced change of channel current consistently on all the inside-out patches and the change remained after the substrates were washed away.

When 4-CY was perfused to patches expressing only Kv1.4, the rate of channel inactivation changed slightly from 35 ± 2.3 to 34 ± 2.7 sec^{-1} (Figure 4B and E, and Table 1; n=10 patches from 4 batches of oocytes), and the current level remained essentially unchanged, indicating that the substrates modulate channel function through Kvβ.

To find out if the change in channel function is due to the redox reaction on Kvβ, we tested 4-CY on Kv1.4 co-expressed with either the D85N or the K118M mutant Kvβ2. In the case of Kv1.4 paired with the D85N mutant, the inactivation rate constant changes from 61 ± 4.1 to 58 ± 4.0 sec^{-1} (Figure 4C and E, and Table 1; n=9, 4 batches of oocytes). In the case of Kv1.4 paired with the K118M Kvβ2, it changes from 59 ± 2.4 to 57 ± 2.5 sec^{-1} (Figure 4D and E, and Table 1; n=6, 3 batches of oocytes). In both cases, 4-CY only induced a small change in channel current level, and altered the rate of inactivation slightly, indicating that 4-CY is less efficient in modulating channel inactivation when the mutant Kvβ is present. Combined, the electrophysiological studies indicate that the substrates modulate channel functions through Kvβ2, and most likely through inducing the redox reaction.

Oxidation of the bound NADPH modulates channel function

How does a Kvβ substrate modulate channel function? On an excised patch, Kvβ very likely contains an NADPH and when a substrate is applied to the patch, the Kvβ2-bound NADPH is oxidized. The NADPH-to-$NADP^+$ conversion induces a change in channel inactivation. If this hypothesis is true, we can make the following two predictions and test them experimentally.

First, we reasoned that perfusing a patch with NADPH after channel modulation should reverse the 4-CY/4-CB effect because it would reload Kvβ2 with the reduced cofactor. Indeed the 4-CY effect was slowly reversed when the patch was perfused with 0.2mM of NADPH (Figure 4F, the left panel). Recovery of current was observed in all the patches (n=8), and in two of them the current recovered to the level before 4-CY application. In sharp contrast, no change in channel current was observed when NADPH was perfused to patches (n=5) expressing Kv1.4 only (Figure 4F, the right panel). These experiments suggest that Kvβ on an inside-out patch can complete an enzymatic cycle, when 4-CY was perfused to oxidize its bound cofactor, and followed by fresh NADPH to re-prime the enzyme. Changes in channel function served as a readout.

Second, we found that when a patch expressing both Kv1.4 and Kvβ2 was exposed to a substrate, channel current increases gradually over time and reaches a steady-state (Figure 5A). This suggests that although we do not know how the NADPH-to-$NADP^+$ conversion induces a change in channel current, we can nevertheless follow the time course of channel modulation by measuring the current level as a function of time after a substrate was applied. Since 4-CB reacts with the bound NADPH at a rate ~3 fold slower than 4-CY (Figure 2C), we predict that channel modulation by 4-CB may also be slower if the cofactor oxidation is required for channel modulation. To test this prediction, we measured channel modulation using 4-CY and 4-CB, both at 5mM concentration. Shown in Figure 5B are the fractions of the total current change plotted versus substrate exposure time. The data points were well fit by single exponential functions (Figure 5B, solid curves), with a time constant of 8.5 ± 0.4 minute (8 patches) and 2.6 ± 0.2 minute (11 patches), for 4-CB and 4-CY, respectively. Therefore 4-CY modulates channel function at ~3 fold faster than 4-CB, similar to the difference observed in the hydride

transfer reaction. This result strongly supports the notion that channel modulation is induced by the Kvβ bound NADPH-to-$NADP^+$ conversion.

Faster hydride transfer rate when Kvβ is assembled with Kv1

Since the patch clamp studies were done at room temperatures (20-23°C), we then measured the hydride transfer reaction at 22°C so that the time constant of channel modulation can be directly compared to that of NADPH consumption in a test tube. We found that 5mM 4-CB and 4-CY oxidized the Kvβ2-bound NADPH with a time constant of 19.8 ± 0.3 minute (n=3) and 6.0 ± 0.1 minute (n=3), respectively. Both time constants are ~2.5 fold larger than these measured at 37°C so that 4-CY remains ~3 fold faster than 4-CB in oxidizing the NADPH. Compared to the time constants of channel modulation, both time constants are larger than these measured in patch clamp studies. It is likely that the hydride transfer rate is faster on a patch presumably because Kvβ is now assembled with a Kv1 channel, although we cannot rule out other possibilities, for example, Kvβ expressed in an oocyte may have different kinetic properties from that expressed in bacteria.

DISCUSSION

In this study, we have demonstrated that Kvβ is a functional AKR, and we have shown that Kvβ substrates modulate channel inactivation through oxidizing the bound NADPH cofactor. These results indicate that the functions of the two proteins are dynamically coupled. It is well-known that co-expression of Kvβ with Kv1 channels increases channel surface expression level ([26,34]), and alters kinetic properties of channel activation and inactivation([25,35-37]). With the demonstration that Kvβ is a functional enzyme, it is now possible to test if other aspects of channel functions are coupled to the AKR activity as well.

In a generic AKR, there are four highly conserved catalytic residues (Figure 1B). Of the four, the catalytic aspartate, tyrosine, and lysine are almost 100% conserved among all AKR families including Kvβ, while the histidine is conserved in some of the AKR families and in Kvβ it is a glutamine. In a 3α-HSD when the histidine was mutated to a glutamate, it has little impact on the turnover rate constant but increased the Km by a factor of 10([38]). Similarly, mutating the histidine to an asparagine in an aldehyde reductase reduced the turnover rate constant by only a factor of 3, but substantially increased the Km value of the substrates([39]). These results indicate that the histidine residue may play an important role in substrate recognition, and is consistent with high Km value we obtained for Kvβ. The corresponding glutamine residue in Kvβ could be evolved for the recognition of its specific native substrate.

The multiple enzymatic turnover rate constant of Kvβ2 is ~0.08 $minute^{-1}$, and is almost the same for the two substrates. In comparison, 3α-HSD catalyzes a very similar substrate, 4-nitrobenzaldehyde, at a rate of 61.4 $minute^{-1}$([40]), almost 760 fold faster than Kvβ2. On the other hand, the single turnover rate constant of Kvβ is at least 1.9 $minute^{-1}$. Compared to a 3α-HSD, the native substrate 5α-dihydrotestosterone oxidizes the bound NADPH at a limiting rate of 26 $minute^{-1}$([41]), which is ~14 fold faster than Kvβ. These results indicate that Kvβ is a slow enzyme mainly because it has a slow cofactor exchange rate.

Is Kvβ a redox sensor that detects change in cellular chemistry and modulates channel function, or an enzyme whose catalytic activity is regulated by channel activities? Data presented here cannot distinguish between the two possibilities, but seem to favour somewhat the redox sensor mechanism. The enzymatic turnover rate constant appears too slow if the function of Kvβ is to catalyze substrate turnover, but not so if it is to sense cellular redox changes, which would require only the hydride transfer step and occurs over the time scale consistent with our experiments. Furthermore, earlier structural studies have shown that the bound NADPH was oxidized over a period of two weeks during the crystallization process, but nevertheless the

$NADP^+$ still was present in the structure of Kvβ2([10]). The tight association is partly due to a flexible loop stretching over the NADPH binding site and restricting the dissociation of the cofactor (marked in yellow in Figure 1B)([3,10,11]). The structure of Kvβ suggests that the tight Kvβ-NADPH complex is built to respond to a redox signal quickly and keep the channel in a modulated state for a prolonged period of time. Consistent with this, Kvβ has been implicated in channel modulation during oxidative stress and hypoxic conditions, and we have found that 4-oxo-nonenal, a lipid peroxidation product generated during oxidative stress([42,43]), oxidizes the Kvβ-bound NADPH and also modulates channel functions in a similar way (data not shown). However, a definitive answer to the question will require understanding the detailed mechanisms of the functional coupling, and discovering the physiological substrate(s) of Kvβ.

The functional interactions between the two proteins demonstrate a simple way of coupling intracellular redox states to a cell's excitability. The results presented here bring us one step forward to understanding the physiological functions of Kvβ.

Acknowledgments

We thank Dr. R. MacKinnon for his advices and generous help. We thank Dr. T. Penning for advices on AKR structure-function, and for providing the 3α-HSD protein. We thank Drs. C. Deutsch, S. Marx, C. Miller, and G. Pitt for critical comments on the manuscript. Finally, we thank J. Riley for expert technical assistance. This work was supported by awards to M.Z. from the National Multiple Sclerosis Society (Pilot Research Award), the March of Dimes Birth Defects Foundation (research grant #5-FY06-20), the American Heart Association (SDG 0630148N), and the US National Institutes of Health (HL086392).

REFERENCES

1. Parcej DN, Scott VE, Dolly JO. Biochemistry 1992;31:11084–11088. [PubMed: 1445846]
2. Scott VE, Rettig J, Parcej DN, Keen JN, Findlay JB, Pongs O, Dolly JO. Proc. Natl. Acad. Sci. U. S. A 1994;91:1637–1641. [PubMed: 8127858]
3. Long SB, Campbell EB, MacKinnon R. Science 2005;309:897–903. [PubMed: 16002581]
4. Sewing S, Roeper J, Pongs O. Neuron 1996;16:455–463. [PubMed: 8789960]
5. Yu W, Xu J, Li M. Neuron 1996;16:441–453. [PubMed: 8789959]
6. Heinemann SH, Rettig J, Wunder F, Pongs O. FEBS Lett 1995;377:383–389. [PubMed: 8549760]
7. Schultz D, Litt M, Smith L, Thayer M, McCormack K. Genomics 1996;31:389–391. [PubMed: 8838324]
8. McCormack T, McCormack K. Cell 1994;79:1133–1135. [PubMed: 8001150]
9. Hyndman D, Bauman DR, Heredia VV, Penning TM. Chem. Biol. Interact 2003;143-144:621–631. [PubMed: 12604248]
10. Gulbis JM, Mann S, MacKinnon R. Cell 1999;97:943–952. [PubMed: 10399921]
11. Gulbis JM, Zhou M, Mann S, MacKinnon R. Science 2000;289:123–127. [PubMed: 10884227]
12. Haddad GG, Jiang C. Annu. Rev. Physiol 1997;59:23–42. [PubMed: 9074755]
13. Haddad GG, Liu H. Adv. Exp. Med. Biol 2000;475:441–452. [PubMed: 10849685]
14. Liu Y, Gutterman DD. Clin. Exp. Pharmacol. Physiol 2002;29:305–311. [PubMed: 11985541]
15. Rozanski GJ, Xu Z. Clin. Exp. Pharmacol. Physiol 2002;29:132–137. [PubMed: 11906472]
16. Coppock EA, Martens JR, Tamkun MM. Am. J. Physiol Lung Cell Mol. Physiol 2001;281:L1–12. [PubMed: 11404238]
17. Patel AJ, Honore E. Eur. Respir. J 2001;18:221–227. [PubMed: 11510795]
18. Jez JM, Bennett MJ, Schlegel BP, Lewis M, Penning TM. Biochem. J 1997;326(Pt 3):625–636. [PubMed: 9307009]
19. Askonas LJ, Ricigliano JW, Penning TM. Biochem. J 1991;278(Pt 3):835–841. [PubMed: 1898369]
20. Grimshaw CE, Shahbaz M, Jahangiri G, Putney CG, McKercher SR, Mathur EJ. Biochemistry 1989;28:5343–5353. [PubMed: 2550052]

21. Kubiseski TJ, Hyndman DJ, Morjana NA, Flynn TG. J. Biol. Chem 1992;267:6510–6517. [PubMed: 1551865]
22. Liu SQ, Jin H, Zacarias A, Srivastava S, Bhatnagar A. J. Biol. Chem 2001;276:11812–11820. [PubMed: 11278398]
23. Ruppersberg JP, Stocker M, Pongs O, Heinemann SH, Frank R, Koenen M. Nature 1991;352:711–714. [PubMed: 1908562]
24. Castellino RC, Morales MJ, Strauss HC, Rasmusson RL. Am. J. Physiol 1995;269:H385–H391. [PubMed: 7631872]
25. Heinemann SH, Rettig J, Graack HR, Pongs O. J. Physiol (Lond) 1996;493(Pt 3):625–633. [PubMed: 8799886]
26. Accili EA, Kuryshev YA, Wible BA, Brown AM. J. Physiol 1998;512(Pt 2):325–336. [PubMed: 9763623]
27. Rasmusson RL, Morales MJ, Castellino RC, Zhang Y, Campbell DL, Strauss HC. J. Physiol 1995;489 (Pt 3):709–721. [PubMed: 8788936]
28. Tseng-Crank J, Yao JA, Berman MF, Tseng GN. J. Gen. Physiol 1993;102:1057–1083. [PubMed: 7907648]
29. Hoshi T, Zagotta WN, Aldrich RW. Science 1990;250:533–538. [PubMed: 2122519]
30. Pardo LA, Heinemann SH, Terlau H, Ludewig U, Lorra C, Pongs O, Stuhmer W. Proc. Natl. Acad. Sci. U. S. A 1992;89:2466–2470. [PubMed: 1549610]
31. Tarle I, Borhani DW, Wilson DK, Quiocho FA, Petrash JM. J. Biol. Chem 1993;268:25687–25693. [PubMed: 8245005]
32. Schlegel BP, Jez JM, Penning TM. Biochemistry 1998;37:3538–3548. [PubMed: 9521675]
33. Weir EK, Lopez-Barneo J, Buckler KJ, Archer SL. N. Engl. J. Med 2005;353:2042–2055. [PubMed: 16282179]
34. Shi G, Nakahira K, Hammond S, Rhodes KJ, Schechter LE, Trimmer JS. Neuron 1996;16:843–852. [PubMed: 8608002]
35. Rettig J, Heinemann SH, Wunder F, Lorra C, Parcej DN, Dolly JO, Pongs O. Nature 1994;369:289–294. [PubMed: 8183366]
36. Accili EA, Kiehn J, Yang Q, Wang Z, Brown AM, Wible BA. J. Biol. Chem 1997;272:25824–25831. [PubMed: 9325312]
37. Morales MJ, Castellino RC, Crews AL, Rasmusson RL, Strauss HC. J. Biol. Chem 1995;270:6272–6277. [PubMed: 7890764]
38. Penning TM, Ma H, Jez JM. Chem. Biol. Interact 2001;130-132:659–671. [PubMed: 11306084]
39. Barski OA, Gabbay KH, Grimshaw CE, Bohren KM. Biochemistry 1995;34:11264–11275. [PubMed: 7669785]
40. Jez JM, Schlegel BP, Penning TM. J. Biol. Chem 1996;271:30190–30198. [PubMed: 8939970]
41. Heredia VV, Penning TM. Biochemistry 2004;43:12028–12037. [PubMed: 15379543]
42. Rindgen D, Nakajima M, Wehrli S, Xu K, Blair IA. Chem. Res. Toxicol 1999;12:1195–1204. [PubMed: 10604869]
43. Lee SH, Blair IA. Chem. Res. Toxicol 2000;13:698–702. [PubMed: 10956056]

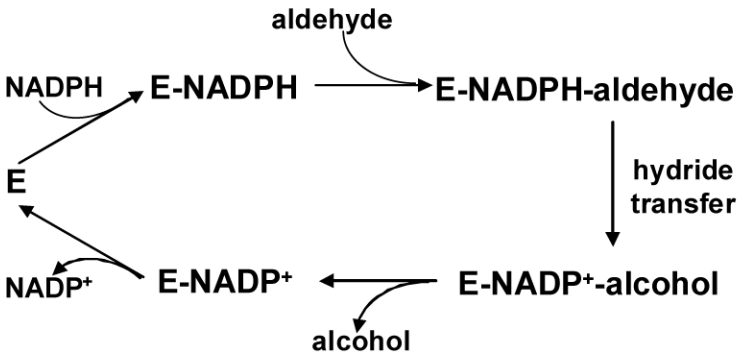

Scheme 1.

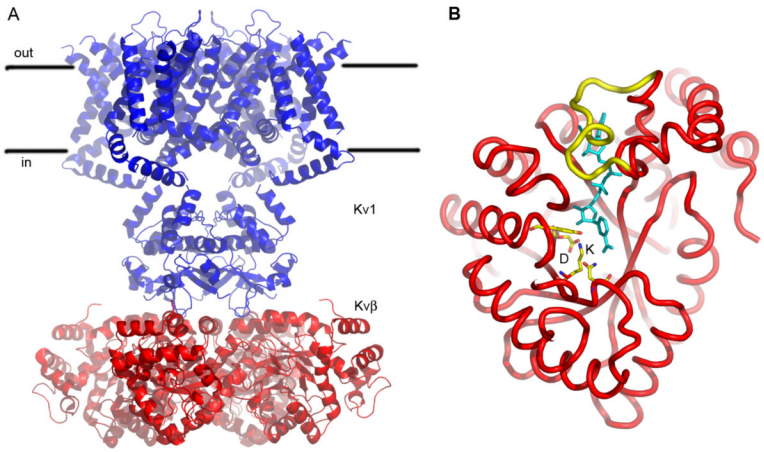

Figure 1. Structural features of Kvβ

A. Structure of Kv1.2 (blue) in complex with Kvβ2 (red) in ribbon representation (pdb code 2A79([3])). Cell membrane is indicated by the straight lines. **B.** Ribbon representation of Kvβ2 showing its structural fold (pdb code 1QRQ([10])). The bound cofactor (cyan) and the conserved active site residues, D85, Y90, K118, and N158, are shown in stick representation. Residues D85 and K118 are labeled. A flexible loop that straddles the cofactor binding site is shown in yellow. The figure was generated using Pymol (www.pymol.org).

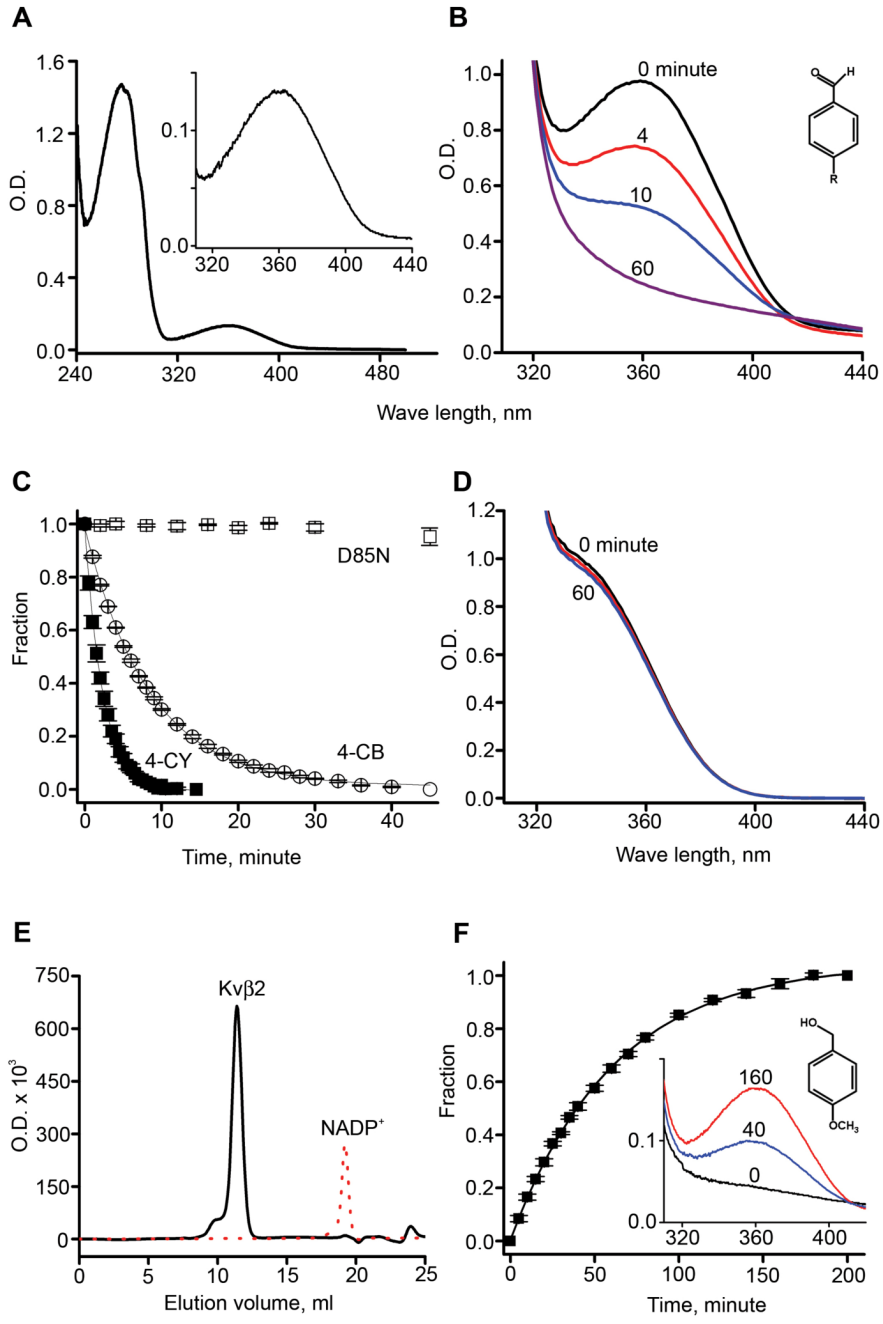

Figure 2. Enzymatic properties of Kvβ2

A. A UV Spectrum of freshly purified Kvβ2 protein. The peak at 363nm is magnified in the inset. **B.** UV spectra taken at the marked time point after mixing Kvβ2 protein with 5 mM 4-CB. The chemical structures of 4-CB (R=COOH) and 4-CY (R=CN) are shown in the inset. **C.** Fraction of the 363nm peak remaining plotted versus time for the wild type (4CB (○) and 4CY (■)) and the D85N mutant (□) Kvβ2. The smooth curves are single-component exponential functions fit to the data. Error bars are s.e.m of 5 (wild type, 4-CB), 6 (wild type, 4-CY), and 3 (D85N) independent experiments. **D.** UV spectra taken at 0 (black trace), 30 (red trace), and 60 (blue trace) minute(s) after mixing 5mM 4-CB with NADPH. **E.** Gel filtration elution profiles for oxidized Kvβ2 (black trace) and for $NADP^+$ alone (red trace). The molar

ratio of Kvβ2 to $NADP^+$ is kept at 1:1. UV absorption was monitored at 254nm where $NADP^+$ has a prominent absorption peak. **F.** Fraction of the total 363nm peak plotted versus time after the oxidized Kvβ was mixed with 10mM 4-MOB. Inset: UV spectra of oxidized Kvβ2 taken at the different time point after mixing with 4-MOB. The chemical structure of 4-MOB is shown to the right.

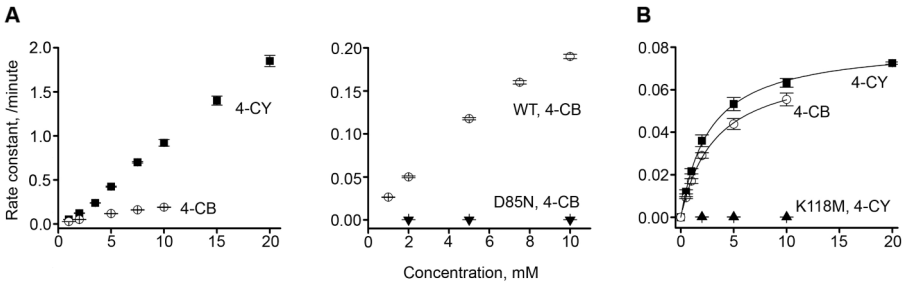

Figure 3. Kinetic studies of Kvβ2

A. Left panel, rate constants of the hydride transfer reaction plotted versus 4-CB (○) or 4-CY (■) concentrations. Right panel, the rate constant of the hydride transfer reaction for 4CB on wild type (○) or the D85N mutant (▼) Kvβ2. Notice that the scale of the y axis is different. Error bars are s.e.m of 3-8 independent experiments. **B.** Steady-state turnover rates constant plotted versus substrate concentrations. ○, 4-CB on the wild type Kvβ; ■, 4-CY on the wild type Kvβ2; and ▲, 4-CY on the K118M mutant Kvβ2. The smooth curves are fitting of the data points with a Michaelis-Menten equation. Error bars are s.e.m of 3-5 independent experiments.

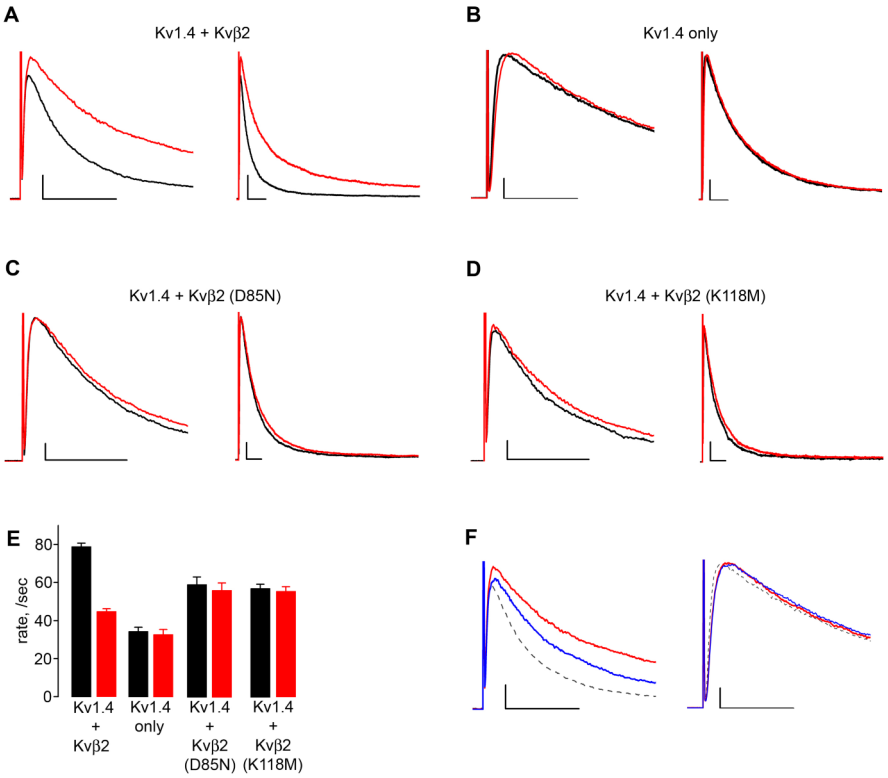

Figure 4. Channel modulations by Kvβ substrates

A-D. Current traces of Kv1.4 expressed with no Kvβ2 (**B**), with the wild type Kvβ2 (**A**), with the D85N Kvβ2 (**C**), and with the K118M Kvβ2 (**D**). In each case, current traces at two different time scales are shown. The black trace was recorded before 4-CY application. After incubating the patch for 10 minutes in the internal solution containing 5mM 4-CY, the solution was exchanged to wash away 4-CY, and the red trace was recorded. **E.** Channel inactivation rate before (black) and after (red) 4-CY application. The error bars are s.e.m of 31 (for 1.4 +Kvβ2), 10 (for Kv1.4 alone), 9 (for Kv1.4+D85N Kvβ2), and 6 (for Kv1.4+K118M Kvβ2) independent measurements (patches). **F.** The same experiments shown in **A**. After recording the red trace, the bath solution was exchanged to the one containing 0.2mM NADPH and the blue trace was recorded 30 minutes after incubation. Potassium currents in both Figure 4 and 5 were recorded from inside-out patches. Currents were elicited by holding the patches at −100mV for at least 30 seconds and stepping to +60mV for 500 miliseconds. All scale bars represent 200 pA and 20 msec.

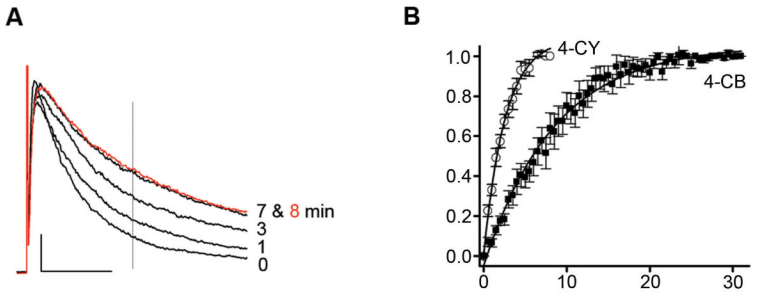

Figure 5. Channel modulation rate on a patch

A. Current traces of Kv1.4 co-expressed with Kvβ2 recorded at the indicated 4-CY exposure time. The dotted line indicates the time point, 30 msec after the pulse, where the current amplitudes were taken for further analysis (in **B**). After 7 minutes, channel current essentially reaches a steady state. **B.** Fraction of current change plotted versus substrate exposure time for 4-CB (■) and 4-CY (○). The smooth curves are single-component exponential functions fit to the data points. Error bars represent s.e.m of 8 (4-CB) and 11 (4-CY) independent measurements (patches).

Table 1

Inactivation time constants for Kv1.4 channels paired with different Kvβ2s.
Current decay was fit with an exponential function with two components, τ1 and τ2. The fraction of each component is *f*1 and *f*2, respectively. The Kv1.4 used in this study has a cysteine at position 13 mutated to a serine (see Methods).

	τ1 (msec)	***f*1**	**τ2 (msec)**	***f*2**
Kv1.4	28.2 ± 1.8	0.54 ± 0.061	75.1 ± 2.7	0.46 ± 0.061
Kv1.4 (after 4-CY)	29.6 ± 2.4	0.61 ± 0.054	76.8 ± 3.9	0.39 ± 0.054
Kv1.4 + Kvβ2	12.3 ± 0.28	0.81 ± 0.013	46.6 ± 2.2	0.19 ± 0.012
Kv1.4 + Kvβ2 (after 4-CY)	21.7 ± 0.68	0.74 ± 0.021	86.4 ± 5.5	0.26 ± 0.021
Kv1.4 + Kvβ2 D85N	16.4 ± 1.1	0.80 ± 0.023	57.5 ± 8.0	0.20 ± 0.023
Kv1.4 + Kvβ2 D85N (after 4-CY)	17.3 ± 1.2	0.80 ± 0.031	57.8 ± 7.8	0.20 ± 0.030
Kv1.4 + Kvβ2 K118M	17.0 ± 0.68	0.64 ± 0.054	62.9 ± 3.7	0.36 ± 0.054
Kv1.4 + Kvβ2 K118M (after 4-CY)	17.5 ± 0.76	0.71 ± 0.055	63.2 ± 7.9	0.29 ± 0.055